

# Arrays of lipid bilayers and liposomes on patterned polyelectrolyte templates

Neeraj Kohli<sup>1</sup>, Sachin Vaidya<sup>1</sup>, Robert Y. Ofoli, Robert M. Worden, Ilsoon Lee\*

*Department of Chemical Engineering and Materials Science, Michigan State University, East Lansing, MI 48824, USA*

Received 8 March 2006; accepted 8 May 2006

Available online 27 May 2006

## Abstract

This paper presents novel methods to produce arrays of lipid bilayers and liposomes on patterned polyelectrolyte multilayers. We created the arrays by exposing patterns of poly(dimethyldiallylammonium chloride) (PDAC), polyethylene glycol (m-dPEG) acid, and poly(allylamine hydrochloride) (PAH) on polyelectrolyte multilayers (PEMs) to liposomes of various compositions. The resulting interfaces were characterized by total internal reflection fluorescence microscopy (TIRFM), fluorescence recovery after pattern photobleaching (FRAPP), quartz crystal microbalance (QCM), and fluorescence microscopy. Liposomes composed of 1,2-dioleoyl-*sn*-glycero-3-phosphocholine (DOPC) and 1,2-dioleoyl-*sn*-glycero-3-phosphate (monosodium salt) (DOPA) were found to preferentially adsorb on PDAC and PAH surfaces. On the other hand, liposome adsorption on sulfonated poly(styrene) (SPS) surfaces was minimal, due to electrostatic repulsion between the negatively charged liposomes and the SPS-coated surface. Surfaces coated with m-dPEG acid were also found to resist liposome adsorption. We exploited these results to create arrays of lipid bilayers by exposing PDAC, PAH and m-dPEG patterned substrates to DOPA/DOPC vesicles of various compositions. The patterned substrates were created by stamping PDAC (or PAH) on SPS-topped multilayers, and m-dPEG acid on PDAC-topped multilayers, respectively. This technique can be used to produce functional biomimetic interfaces for potential applications in biosensors and biocatalysis, for creating arrays that could be used for high-throughput screening of compounds that interact with cell membranes, and for probing, and possibly controlling, interactions between living cells and synthetic membranes.

© 2006 Elsevier Inc. All rights reserved.

**Keywords:** Polyelectrolytes; Liposomes; Lipid bilayers; BLM; Total internal reflection fluorescence microscopy (TIRFM); Fluorescence recovery after pattern photobleaching (FRAPP); Quartz crystal microbalance (QCM); Fluorescence microscopy; Microarray

## 1. Introduction

Cell membranes are complex moieties composed primarily of a bilayer lipid membrane (BLM) and associated membrane proteins. These membranes represent one of the major structural components of cells and are responsible for many vital cellular functions. Biomimetic interfaces that can mimic cell membranes and their functionalities have potential applications as biosensors and can also provide a platform for fundamental investigations of biomolecular behavior [1–5]. To mimic cell membranes, supported BLMs (sBLMs) have been formed on glass, silica and unfunctionalized metal surfaces [4,6–16]. Although sBLMs have enabled researchers to probe properties such as phase transition, lateral diffusion, permeation, and

lipid–protein interactions [17], they have two serious limitations: (1) they do not provide space between the bilayer and the underlying substrate to accommodate hydrophilic moieties of trans-membrane proteins, and to allow lateral mobility of membrane components, and (2) they lack the ionic reservoirs that most cell membranes need to ensure their biological function.

To overcome these limitations, new approaches that involve the use of hydrophilic cushions on which BLMs can be deposited are being adopted by researchers. Such cushions have consisted of hydrogels, polymeric tethers, polymer films and polyelectrolyte multilayers (PEMs) [18–37]. PEMs offer the following advantages [29–34,36]: (1) they are robust and easy to fabricate, (2) they can be deposited on virtually any surface, (3) they can provide a reservoir for electron transfer mediators and cofactors for sensor applications, and (4) their porosity and flexibility may allow the protein to exist in its natural conformation while bound to the BLM. Lipid bilayers composed of negatively charged

\* Corresponding author. Fax: +1 (517) 432 1105.

E-mail address: [leeil@egr.msu.edu](mailto:leeil@egr.msu.edu) (I. Lee).

<sup>1</sup> Equal contributors.

lipids like 1,2-dioleoyl-*sn*-glycero-3-phosphate (monosodium salt) (DOPA), 1-stearoyl-2-oleoyl-phosphatidylserine (SOPS), and 1,2-dimyristoyl-*sn*-glycero-3-[phospho-*rac*-(1-glycerol)] (sodium salt) (DMPG) blended with other zwitterionic lipids like 1,2-dioleoyl-*sn*-glycero-3-phosphocholine (DOPC) and 1-palmitoyl-2-oleoylphosphatidylcholine (POPC) have already been shown to form on polyelectrolytes such as poly(allylamine hydrochloride) (PAH), poly(ethyleneimine) (PEI) and poly(diallyldimethyl ammonium chloride) (PDAC) coated substrates [29,33,34,36,38,39]. These studies [29] have shown that, upon increasing the percentage of charged lipids, lipid coverages increase, and diffusion coefficients decrease. In another approach [40], PEMs were adsorbed on melamine formaldehyde latex particles which were soluble at low pH, resulting in the formation of thin polyelectrolyte shells upon dissolving the core. Lipid bilayers were then formed on the empty shells by exposing them to charged vesicles. The properties of this system as an artificial cell were then evaluated.

Arrays of BLMs have also been fabricated on glass and gold surfaces [26,33,41–48]. In one approach, a patterned poly(dimethyl siloxane) (PDMS) stamp was brought into contact with an sBLM formed on a glass slide and then removed [41]. Approximately 90% of the lipids in areas in contact with the stamp were transferred to the stamp's surface, resulting in arrays of BLM patches separated from one another by regions of bare glass. The same group showed that the bilayer can be preassembled directly onto oxidized PDMS surfaces and then transferred intact to the glass slide. Bilayer patches in the resulting arrays were found to be fully fluid and stable under water. To date, this methodology has been applied only to a limited number of surfaces.

There is general interest in techniques that can help extend these types of approaches to other substrates, and also address the two limitations of sBLMs described earlier. The approach in this study is based on the ionic layer-by-layer (LBL) assembly technique introduced by Decher and Hong [49], microcontact printing ( $\mu$ CP) developed by the Whitesides group [50], and the polymer-on-polymer stamping process (POPS) developed by Hammond and coworkers [51,52]. LBL assembly can be used to deposit PEMs on most substrates. PEMs are thin films [49] formed by electrostatic interactions between oppositely charged polyelectrolyte species to create alternating layers of sequentially adsorbed ions. They are economical to produce, and have been effectively used as functional polymers [53], colloids [54–56], biomaterials [57] and templates for selective electroless metal deposition [58]. Microcontact printing [50] is a soft lithographic technique used in physics, chemistry, materials science and biology to transfer patterned thin organic films to surfaces, with sub-micron resolution. Unlike other fabrication methods that merely provide topographic contrast between the feature and the background,  $\mu$ CP also allows chemical contrast to be achieved via selection of an appropriate ink. Microcontact printing offers advantages over conventional photolithographic techniques because it is simple to perform and is not diffraction-limited. This technique has been used to make patterns of various small and large molecules on metals and silicon substrates [59–62], as well as to deposit proteins [63] and

polyelectrolyte aggregates [64]. POPS is an approach that combines LBL assembly and  $\mu$ CP to generate alternating regions of different chemical functionalities on a surface by using graft, diblock copolymers or polyelectrolytes as ink [51,52].

In this paper, we present methods to fabricate arrays of BLMs and liposomes on PEMs. Arrays of BLMs were created by exposing PDAC patterns, polyethylene glycol (m-dPEG acid) patterns, and PAH patterns on PEMs to liposomes of various compositions. Total internal reflection fluorescence microscopy (TIRFM) and quartz crystal microbalance (QCM) gravimetry were used to monitor liposome adsorption to PEMs. Fluorescence recovery after pattern photobleaching (FRAPP) and fluorescence microscopy were also used to characterize the resulting interfaces.

## 2. Materials and methods

### 2.1. Materials

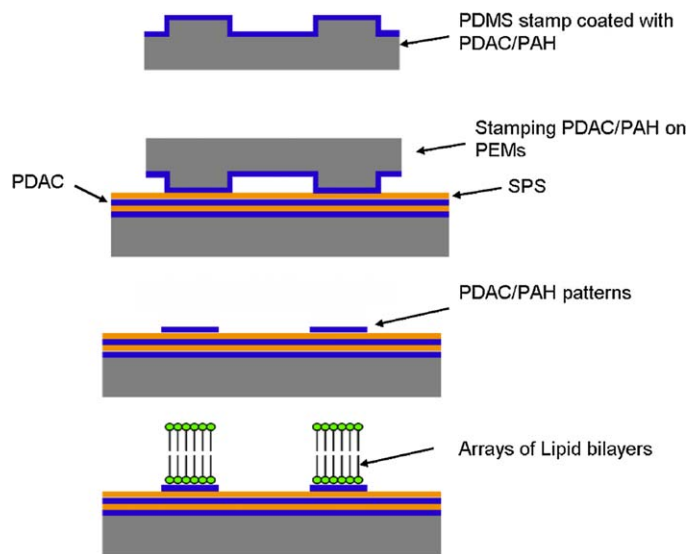
Sulfonated poly(styrene) (SPS) ( $M_w \sim 70,000$ ), poly(diallyldimethyl ammonium chloride) (PDAC) ( $M_w \sim 100,000$ ), and poly(allylamine hydrochloride) (PAH) were obtained from Sigma (St. Louis, MO). 1,2-dioleoyl-*sn*-glycero-3-phosphate (monosodium salt), 1,2-dioleoyl-*sn*-glycero-3-phosphocholine (DOPC), and 1-palmitoyl-2-[6-[(7-nitro-2-1,3-benzoxadiazol-4-yl)amino]hexanoyl]-*sn*-glycero-3-phosphocholine (16:0-06:0 NBD-PC) were purchased from Avanti Polar Lipids (Alabaster, AL). NBD-PC serves as the fluorescence probe. 1-tetradecanethiol, 4-(2-hydroxyethyl)piperazine-1-ethanesulfonic acid sodium salt (HEPES) was obtained from Fluka (St. Louis, MO). The m-dPEG acid was purchased from Quanta Biosign (Powell, OH). Sylgard 184 silicone elastomer kit (Dow Corning, Midland MI) was used to prepare the poly(dimethylsiloxane) (PDMS) stamps for  $\mu$ CP. The fluorosilanes were purchased from Aldrich Chemical (St. Louis, MO). Ultrapure water (18.2 M $\Omega$ ) was supplied by a Nanopure-UV four-stage purifier (Barnstead International, Dubuque, IA); the purifier was equipped with a UV source and a final 0.2  $\mu$ m filter.

### 2.2. Preparation of stamps

The PDMS stamps were made by pouring a 10:1 solution of elastomer and initiator over a prepared silicon master. The silicon master was pretreated with fluorosilanes to facilitate the removal of the PDMS stamps from the silicon masters. The mixture was allowed to cure overnight at 60 °C. The masters were prepared in the Microsystems Technology Lab at MIT and consisted of features (parallel lines and circles) from 1 to 20  $\mu$ m.

### 2.3. Preparation of liposomes

Small unilamellar liposomes of two different compositions were prepared: (1) 89% DOPC, 10% DOPA and 1% NBD-PC (referred in the paper as 90% DOPC/10% DOPA), (2) 79% DOPC, 10% DOPA and 1% NBD-PC (referred in the paper as 80% DOPC/20% DOPA). These liposomes were prepared by



Scheme 1. Schematic representation of the process for the fabrication of arrays of BLMs on PDAC and PAH patterned substrates.

mixing appropriate amounts of lipids in chloroform. This mixture was then dried under nitrogen, making sure lipid formed a thin, cake-like film on the walls of the test tube. The residual chloroform was removed under high vacuum. The lipids were then reconstituted in 10 mM HEPES buffer (pH 7.4, 100 mM NaCl), and the resulting liposome solution was sonicated until it became clear using a Branson bath sonicator (Branson Ultrasonics Corporation, Danbury, CT).

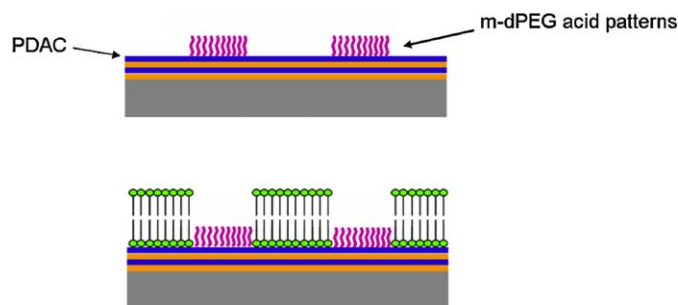
#### 2.4. Preparation of polyelectrolyte multilayers (PEMs)

A Carl Zeiss slide stainer equipped with a custom-designed ultrasonic bath was connected to a computer to perform LBL assembly [54,55,58,65]. For PDAC/SPS and PAH/SPS multilayers, the concentration of SPS, PDAC and PAH solution was 0.01, 0.02 and 0.01 M, respectively, as based on the molecular repeat units. All polyelectrolyte solutions contained 0.1 M NaCl and were at a pH of 7.0. To deposit PEMs, the glass slides were cleaned with a dilute Lysol water mixture in a sonicator. These slides were then dried under  $N_2$  gas and were further cleaned using Harrick plasma cleaner (Harrick Scientific Corporation, Brooding Ossining, NY) for 10 min at 20 Pa. To form the first polyelectrolyte bilayer, the slides were immersed for 20 min in a PDAC (or PAH) solution. Following two sets of 5 min water rinse with agitation, the slides were subsequently placed in a SPS solution for 20 min. They were rinsed again with water, and this process was repeated to build multiple layers.

#### 2.5. Preparation of arrays

Two different schemes were used to prepare arrays of BLMs.

**Scheme 1:** A PDMS stamp was dipped in a 250 mM solution of PDAC (or 200 mM solution of PAH) in 75/25 ethanol–water mixture for about 20 min [51,52]. The stamp was then washed with ethanol, dried under nitrogen and brought in contact with a glass slide that was coated with 5 PDAC/SPS (or PAH/SPS) bilayers, with SPS forming the uppermost layer. The



Scheme 2. Schematic representation of the process for the fabrication of arrays of BLMs on m-dPEG acid patterned substrates.

stamp was removed after 15 min, and the resulting PDAC (or PAH) patterns were then rinsed with water to remove unbound or loosely bound PDAC (or PAH). The stamp was then exposed to DOPC/DOPA liposomes of varying compositions.

**Scheme 2:** A PDMS stamp was dipped in a 100  $\mu$ M solution of m-dPEG acid in a 75/25 ethanol–water mixture for 30 min [66]. The stamp was then washed, dried under nitrogen and brought in contact with the glass slide coated with 4.5 PDAC/SPS multilayers with PDAC as the topmost layer. The stamp was removed after 20 min and the resulting m-dPEG acid patterns were then rinsed with water to remove excess m-dPEG acid. These patterns were then exposed to negatively charged DOPC/DOPA liposomes. All the fluorescence images were obtained using the Nikon Eclipse E 400 microscope (Nikon, Melville, NY) having a filter cube (Ex: 465–495/DM: 505/Em: 515–555).

For slides used in TIRFM, FRAPP and QCM experiments, PEM assemblies were deposited using the sequential approach described above.

#### 2.6. Total internal reflection fluorescence microscopy (TIRFM)

The experimental setup and the flow cell for TIRFM have been described previously [67]. Briefly, the apparatus consists

of an inverted microscope (Zeiss Axiovert 135M, Carl Zeiss Inc. Thornwood, NY), the 488 nm line of a 5 W continuous wave argon ion laser (Lexel Lasers Model 95, Fremont, CA), a side-on photomultiplier tube (Hamamatsu R4632, Bridgewater, NJ) jacketed in a thermoelectrically cooled housing (TE 177-TSRF, Products for Research, Danvers, MA), a CCD camera (NTI, VE1000, Dage-MTI, Michigan City, IN), and a modular automation controller (MAC 2000, Ludl Electronic Products, Hawthorne, NY) that regulates the voltage supply to the photo-multiplier tube and controls translation of the X–Y stage. A double syringe pump system (Model 551382, Harvard Apparatus South Natick, MA) was used for infusion and withdrawal of sample solutions at identical rates from a custom designed flow cell. For measurements that require photon counting, an SR400 photon counter (Stanford Research Systems, Sunnyvale, CA) was used after the output signal from the PMT was amplified by a fast preamplifier (SR445, Stanford Research Systems, Sunnyvale, CA). Fluorescence intensities were recorded using software written in Labview 6.0 (National Instruments, Austin, TX). A 500 nm long-pass band filter was used to separate the excitation and emission wavelengths. An optical chopper (SR 540, Stanford Research Systems, Sunnyvale, CA) was used to prevent unintended photobleaching of fluorophores during experiments. The photon counter was triggered by an output reference voltage from the chopper, so that data collection only occurred during periods when the flow cell was illuminated by the monitoring beam. For TIRFM experiments, the flow cell was initially filled with buffer. Subsequently, a liposome solution was introduced into the flow cell at a controlled flow rate. After filling the flow cell, the infusion was halted, and adsorption was allowed to continue for 1 h, followed by a buffer wash (for desorption experiments or FRAPP experiments). Measurements were done at a temperature of  $22 \pm 1^\circ\text{C}$ , which is above the phase transition temperature of both DOPC ( $-20^\circ\text{C}$ ) and DOPA ( $-8^\circ\text{C}$ ) [68].

### 2.7. Fluorescence recovery after pattern photobleaching (FRAPP)

A system of optical flats [67] was used to toggle between a low intensity monitoring beam for observation of surface dynamics and a high intensity beam for photobleaching purposes. Liposomes were adsorbed on the PEM substrates by flowing liposome solution at a rate of 0.34 ml/min for 10–12 min, using the syringe pump. The infusion was then halted, and adsorption was allowed to continue for approximately 1 h. The flow cell was subsequently flushed with 4–5 flow cell volumes of buffer to remove all free labeled liposomes in the bulk solution. FRAPP experiments were conducted in the flow cell by directing the laser beam through a  $5\times$  beam expander (Edmund Optics Inc., Barrington, NJ), and through a filter cube (Ex: 450–490/DM: 510/Em: 515–565) onto a Ronchi ruling (50 lines per inch, Edmund Optics Inc., Barrington, NJ) which was placed in the back image plane of the microscope to create the fringe pattern on the substrate. Stripe periodicity in the sample plane was  $12.5\ \mu\text{m}$ . An aperture was placed in the image plane in front of the photomultiplier tube to reduce the observation area to a

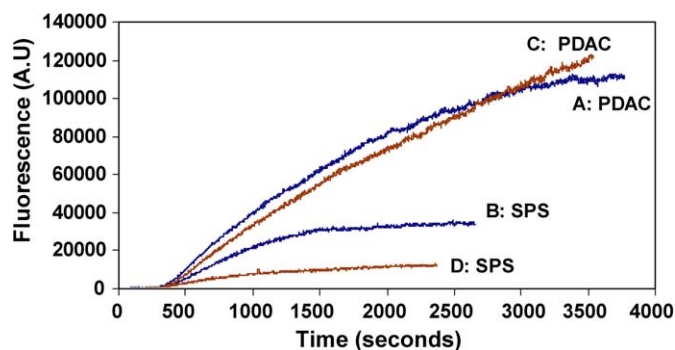


Fig. 1. Adsorption curves of (A) liposomes (10% DOPA, 90% DOPC) on PDAC. (B) liposomes (10% DOPA, 90% DOPC) on SPS. (C) liposomes (20% DOPA, 80% DOPC) on PDAC. (D) liposomes (20% DOPA, 80% DOPC) on SPS.

size smaller than the photobleached area. This was done to ensure that only fluorescence recovery from the unbleached fringe area was monitored (rather than recovery from unbleached areas outside the fringe pattern). All experiments were conducted at  $22 \pm 1^\circ\text{C}$ .

### 2.8. Microgravimetric experiments

A QCM analyzer (5 MHz crystals, Maxtek Inc., Research Quartz Crystal Microbalance, Santa Fe Springs, CA) linked to a computer with RQCM data log software (Maxtek Inc.) was used for microgravimetric measurements. Quartz crystals (Maxtek Inc.) sandwiched between two gold electrodes (geometrical area  $1.26\ \text{cm}^2$ ) were used. The QCM crystals were cleaned in piranha solution (seven parts by volume concentrated sulfuric acid and three parts hydrogen peroxide) for 30 s and then dipped in a 1 mM solution of 3-mercaptopropanoic acid in ethanol for 24 h. PAH/SPS and PDAC/SPS multilayers were then deposited *ex situ* on the crystals according to previously described procedures. Frequency changes of the quartz crystals were measured after obtaining a baseline oscillation frequency change using a 10 mM HEPES buffer (pH 7.4). The measurements were done at  $22 \pm 1^\circ\text{C}$ .

## 3. Results and discussions

### 3.1. Characterization of liposome adsorption by TIRFM

Curves A and B in Fig. 1 depict adsorption of negatively charged liposomes composed of 90% DOPC/10% DOPA to PEMs, with positively charged PDAC and negatively charged SPS as the top layers, respectively. The higher intensities obtained in Curve A indicate that the liposomes adsorbed preferentially onto PDAC, presumably due to electrostatic interactions. To investigate the role of liposome charge on subsequent adsorption, we repeated the experiments with liposomes composed of 80% DOPC and 20% DOPA (Curves C and D in Fig. 1), with PDAC and SPS as the top layer, respectively. The higher concentration of negatively charged lipids (DOPA) in the liposomes further increased the preference of liposomes for PDAC, suggesting that adsorption of liposomes on PEMs is sig-

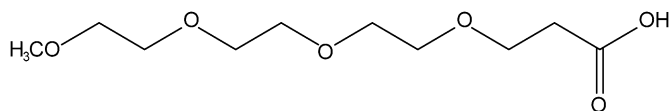


Fig. 2. Structure of m-dPEG acid.

nificantly influenced by electrostatic interactions between the charged lipids and polyelectrolytes.

Curves C and D depict experiments conducted with a separate batch of liposomes from those represented by Curves A and B. Due to variability in liposome characteristics (due to small changes in labeling ratios, etc.), the magnitude of fluorescence emission may vary somewhat from batch to batch. However, unlike the case for Curve A, Curve C for adsorption on PDAC does not appear to approach a saturation value within the duration of the experiment. This may be the result of multilayer deposition at the higher concentrations of DOPA. To avoid the possibility of multilayer formation, liposomes composed of 10% DOPA and 90% DOPC were used for all remaining experiments.

To determine the reversibility of liposome adsorption to PDAC/SPS PEMs, the flow cell was flushed with 3–4 volumes of liposome-free buffer after liposome adsorption. The wash significantly reduced the fluorescence emission when SPS was the top layer, but had a much smaller effect when PDAC was the top layer (data not shown). This result suggests that the lipids are binding more strongly to PDAC than to SPS. It is possible that the buffer wash experiments reflect, in part, depletion of liposomes in the bulk liquid. However, the intensity of the evanescent wave decays exponentially with distance from the interface, and has a penetration depth of only about 80 nm in the TIRFM setup used to conduct these experiments. As a result, illumination of fluorophores in the bulk solution would only make a small contribution to the total fluorescence emission measured. In fact, this interfacial sensitivity allowed TIRFM to monitor liposome adsorption on slides coated with lipid monolayers to show that binding kinetics are strongly influenced by buffer ionic strength [14].

Liposome adsorption on surfaces coated with m-dPEG acid (see structure in Fig. 2) was also studied. Fig. 3a shows liposome adsorption onto PEMs with m-dPEG as the top layer, followed by a wash with liposome free buffer. While some lipids did adsorb onto the m-dPEG acid layers, flushing the flow cell with 3–4 ml of buffer after adsorption resulted in a large decrease in fluorescence for m-dPEG acid coated substrates. This suggests that the liposomes were only loosely bound. By contrast, a buffer wash after approximately 45 min of liposome adsorption produced only a small decrease in fluorescence emission in the case of PEMs topped with PDAC (Fig. 3b).

In the experiments depicted in Fig. 3b, liposome adsorption to PEMs with either PDAC (top curve) or m-dPEG acid (bottom curve) as the topmost layer was halted by introducing buffer (at  $t = 0$  min on the graph), and then the fluorescence emission intensities were monitored to track the process of desorption. To enable direct comparison of the results, the fluorescence emission intensities in each data set were normalized against the corresponding fluorescence emission intensity recorded prior

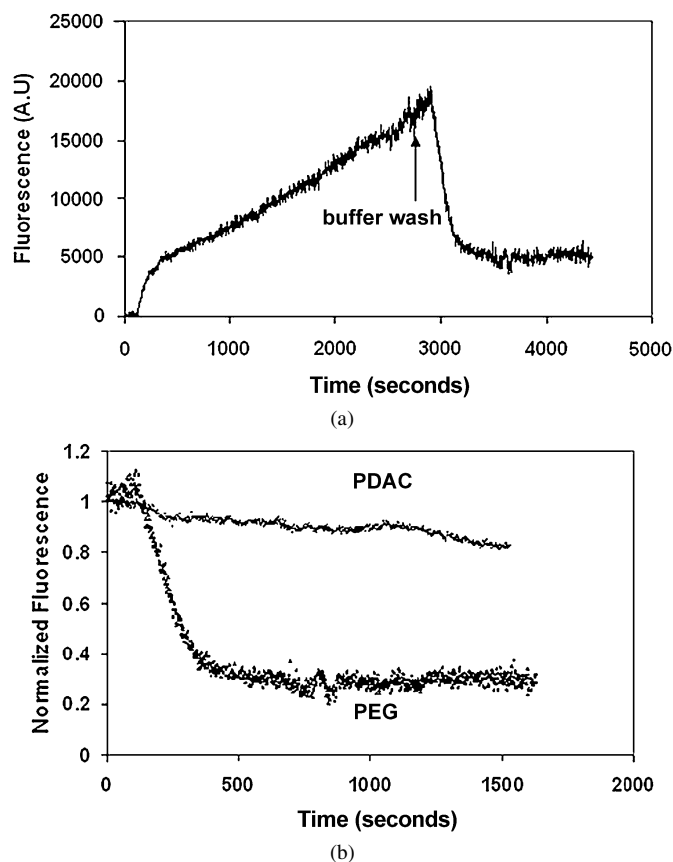


Fig. 3. (a) Adsorption of liposomes (10% DOPA, 90% DOPC) on a glass slide coated with PEMs with m-dPEG acid being the topmost layer. (b) Buffer-wash experiments to study liposome desorption from PEMs. The top and bottom curves depict desorption of liposomes from PEMs with PDAC and m-dPEG as the top layer, respectively. At  $t = 0$ , adsorption of liposomes (which have adsorbed for at least 45 min) is halted by introducing liposome-free buffer. In each curve, the fluorescence intensity has been normalized by the corresponding fluorescence value obtained prior to initiation of the buffer wash.

to initiation of the buffer wash. There was a 70% decrease in the fluorescence emission intensity for the m-dPEG case, compared to a 10% decrease for PDAC. The apparent weakness of liposome adsorption on surfaces coated with both SPS and m-dPEG was confirmed again when fluorescence microscopy was used to characterize arrays of BLMs deposited on patterns of PEMs with PDAC, SPS, and m-dPEG as the topmost layer (results discussed below). While the mechanism by which PEG resists biomolecular adsorption is not completely understood, it is believed to stem either from steric exclusions, which is an entropic effect caused by the unfavorable change in free energy associated with the dehydration and confinement of polymer chains having high conformational flexibility [69], or from long range electrostatic repulsions [70,71]. Previous studies from our group have shown that m-dPEG acid can also resist the adsorption of PDAC, which is a positively charged polyelectrolyte. Therefore, we believe the resistance of m-dPEG acid to negatively charged liposomes stems primarily from steric repulsion.

### 3.2. Formation of arrays of lipid bilayers

Figs. 4a and 4b show fluorescence images of the line and circular patterns, respectively, of liposomes deposited on PDAC.

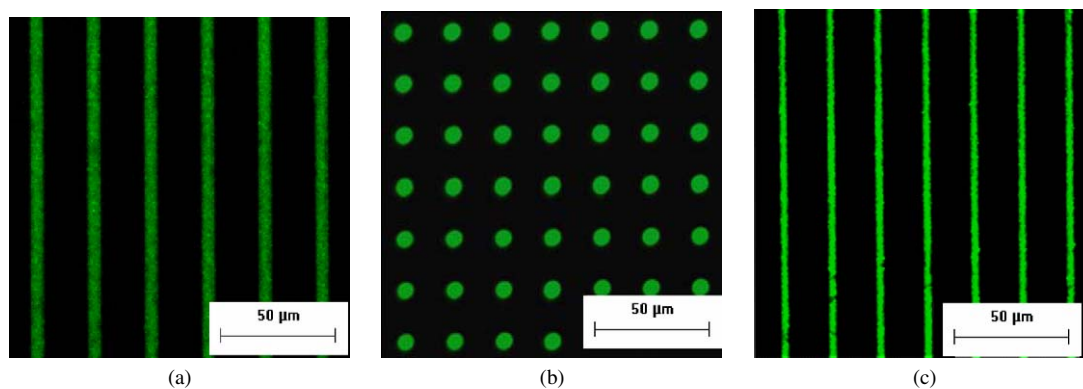


Fig. 4. Fluorescence images showing (a) line patterns on a PDAC patterned substrate, (b) circular patterns on a PDAC patterned substrate, (c) line patterns on a PAH patterned substrate. The ratio of fluorescence intensity between the bright and dark region on PDAC patterned substrate was approximately 45:1.

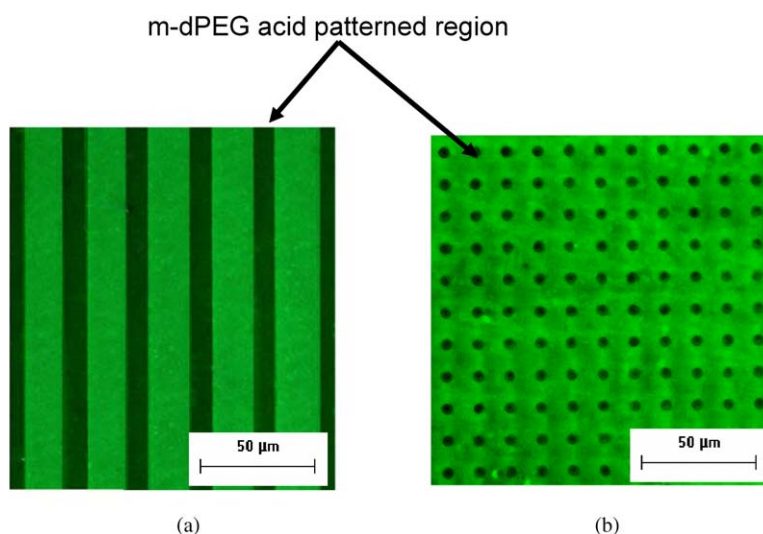


Fig. 5. Fluorescence microscopy images showing (a) line patterns on m-dPEG acid patterned substrate, (b) circular patterns on m-dPEG patterned substrate. The ratio of fluorescence intensity between the bright and dark region was approximately 50:1.

As clearly shown by these results for both linear and circular arrays, liposomes bound preferentially to PDAC (brightly fluorescing features), and negligibly to SPS (dark, featureless background). Similar results were obtained when liposomes were deposited on a surface stamped with a weak polyelectrolyte (PAH) instead of a strong polyelectrolyte (PDAC) on SPS (Fig. 4c). These results are consistent with those obtained during the adsorption experiments (Fig. 1).

In another approach, m-dPEG acid was stamped on a PEM-coated glass slide, with PDAC being the topmost layer. The m-dPEG acid molecule has a carboxylic acid group on one end. At a pH above the  $pK_a$ , the acid group has a negative charge and can be stamped onto PDAC, resulting in patterns of m-dPEG acid on PDAC [66]. Upon subsequent exposure to the liposome solution, liposome adsorption occurred on the exposed PDAC, but not on the m-dPEG acid patterns (Fig. 5). Therefore, the fluorescence patterns in Fig. 5 are the negative replicas of those in Fig. 4. This ability to make either the positive or the negative image of the stamp adds to the versatility of this technique. Similar fluorescence images were obtained when PEM coated glass slides, with PAH being the topmost layer, were used (data not shown).

### 3.3. Assessment of liposome adsorption and rupture to form bilayers

FRAPP was used to determine if the adsorbed liposomes remained intact on the surface or ruptured to form a bilayer. Figs. 6a and 6b show the recovery curves for lipids deposited on PEMs with PDAC and PAH as the topmost layer, respectively. Fluorescence recovery for lipids on PDAC and PAH was adequately described by the single mobile species model, which assumes that there is one population of mobile fluorophores, in addition to an immobile fraction. The equation describing photobleaching recovery in a fringe pattern in such a system is given by Eq. (1) [72,73]

$$f(t) = f(0) + \frac{m}{2} [1 - f(0)] \left[ 1 - \left( \frac{8}{\pi^2} \right) \left\{ \exp\left( -\frac{4\pi^2 Dt}{a^2} \right) + \frac{1}{9} \exp\left( -\frac{36\pi^2 Dt}{a^2} \right) \right\} \right] \quad (1)$$

where  $f(t)$  is the ratio of the postbleach fluorescence ( $t > 0$ ) to the prebleach fluorescence,  $m$  is the fraction of the fluorophores that are mobile and have diffusion coefficient  $D$ , and  $a$

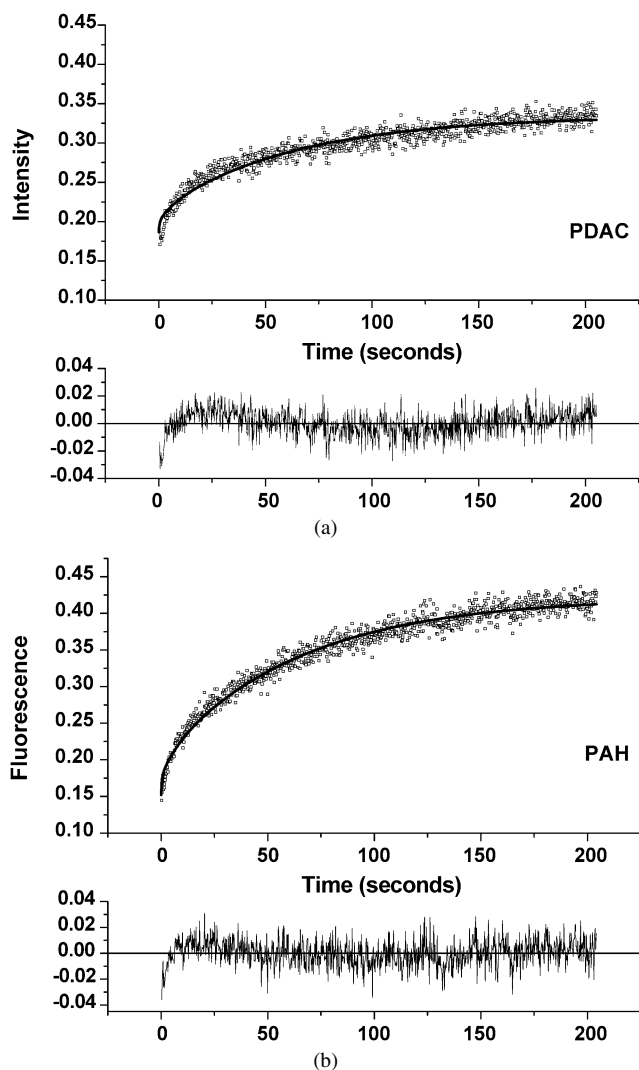


Fig. 6. Fluorescence recovery after pattern photobleaching (FRAPP) profiles on PEMs with (a) PDAC and (b) PAH as topmost layer. Only postbleach fluorescence intensity normalized against the corresponding prebleach fluorescence value is shown. The solid lines in the figures represent fits to the recovery data set with models [72] describing populations with a single mobile fraction and an immobile fraction. Plots of residuals vs time are also indicated below each figure. Average values obtained with these models are summarized in Table 1.

Table 1

Average lipid diffusion coefficients ( $D$ ), and average mobile fractions ( $m$ ) for BLMs formed on PEMs with PDAC and PAH as the topmost layer

Substrate	Average diffusion coefficient ( $\times 10^8$ cm <sup>2</sup> /s)	Average mobile fraction
PAH	$D = 0.056 \pm 0.01$	$m = 0.68 \pm 0.05$
PDAC	$D = 0.072 \pm 0.03$	$m = 0.22 \pm 0.07$

The estimates were obtained by averaging parameters fit from all recovery curves.

is the stripe periodicity in the sample plane. Unlike spot photobleaching, where 100% recovery of fluorophores is possible for a completely formed BLM, only 50% recovery is theoretically possible in FRAPP under the same conditions.

Equation (1) was fit to the FRAPP data, and averages of the best-fit values for  $D$  and  $m$  are summarized in Table 1. The average  $D$  values on PAH and PDAC were comparable

( $0.056 \times 10^{-8}$  and  $0.072 \times 10^{-8}$  cm<sup>2</sup>/s, respectively). For comparison, planar lipid bilayers formed across a pore and natural cell membrane have diffusion coefficients of  $\sim 10^{-7}$  and  $(0.3\text{--}3) \times 10^{-8}$  cm<sup>2</sup>/s, respectively [74]. The average mobile fraction on PAH (0.68) was significantly higher than that on PDAC (0.22). Nollert et al. [75] have described two outcomes when liposomes adsorb to surfaces. In the first, liposomes adsorb but do not rupture. As a result, they produce an immobile fraction because the fluorescently tagged lipids cannot freely migrate between liposomes. In the other scenario, liposomes adsorb, rupture and spread to form sBLMs. Therefore, the higher  $m$  values observed on PAH suggest that adsorbed liposomes more readily ruptured to form a bilayer on PAH than on PDAC. Similar results have been reported in a previously published AFM study which showed that liposomes composed of DOPA adsorb onto a PDAC-coated surface, but most remain intact [76]. On the other hand, liposomes form a continuous sBLM on substrates coated with PEI, which is a weak polyelectrolyte like PAH. However, other feasible mechanisms could also explain the trends seen in Table 1. For instance, lipids adsorbed onto PDAC may form disconnected bilayer patches.

The diffusion coefficients obtained in this study are comparable to those reported for BLM containing SOPS and POPC deposited on PDAC/SPS multilayers ( $0.2 \times 10^{-8}$  cm<sup>2</sup>/s) [33,34]. Our values are, however, lower than those reported for DMPC:DOPA (10:1) BLM deposited on SPS/PAH multilayers [36]. In our system, the dye molecules were present in both the upper and lower leaflet. However, in the reported systems [36] the dye molecule is present only in the upper leaflet and thus they are measuring the diffusion coefficient only of the upper leaflet. The upper leaflet would be less influenced by the underlying substrate and thus would be expected to exhibit a higher diffusion coefficient than the bottom leaflet. Moreover, in our study, NBD was attached to one of the hydrophobic tails of phosphocholine. Cassier et al. have reported that diffusion coefficients can increase by a factor of four if the NBD molecule is attached to the head-group than to the tail of the phosphocholine molecule [36].

### 3.4. Characterization of liposome adsorption and rupture by QCM

QCM has been used effectively to study both kinetics of liposome adsorption and subsequent liposome fusion to form a bilayer [10,77,78]. Adsorption of material onto a QCM chip results in a decrease in the chip's oscillating frequency. Under ideal conditions, there is a linear relationship between the change in the resonant frequency ( $\Delta f$ ) of the QCM chip, and the change in mass ( $\Delta m$ ) due to adsorption:

$$\Delta m = C \frac{\Delta f}{n}, \quad (2)$$

where  $C$  is the mass sensitivity of the crystal, and  $n$  is the overtone number.

The  $\Delta f$  curve corresponding to sBLM formation on silicon dioxide has been shown to have two distinct phases [77]: (1) adsorption of intact liposomes and (2) liposome rupture

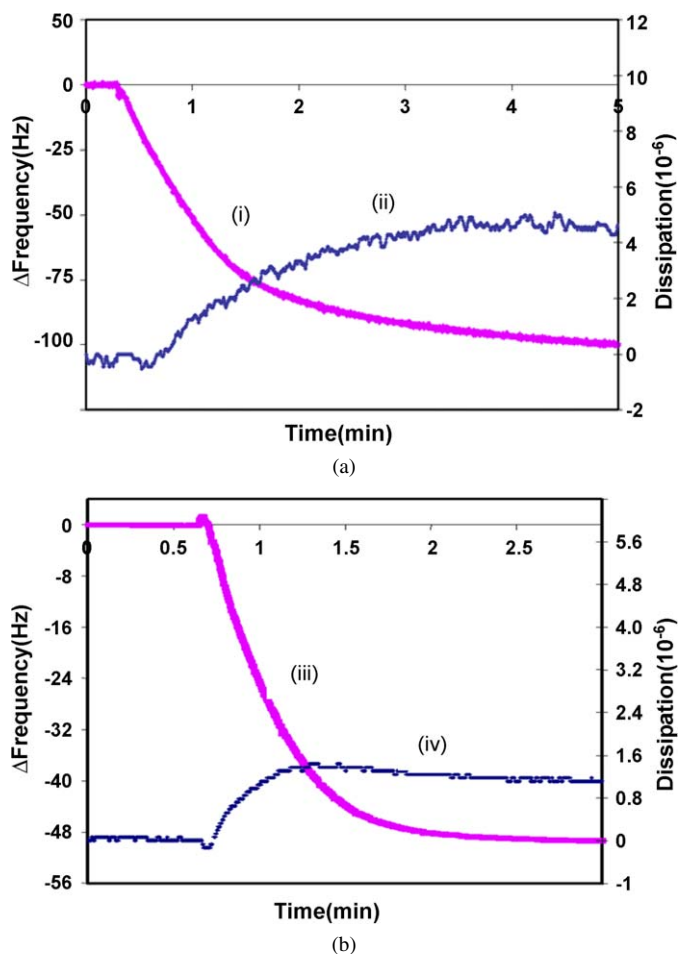


Fig. 7. Changes in QCM resonant frequency (Curves i and iii) and dissipation (Curves ii and iv) versus time for the adsorption of liposomes on (a) PEMs having a top layer of PDAC, (b) PEMs having a top layer of PAH.

and bilayer formation. When adsorbed liposomes rupture, water trapped inside and between them is released, resulting in a loss of adsorbed mass. Thus, Phase 1 is characterized by an increase in mass (decrease in  $f$ ), and Phase 2 is characterized by a subsequent decrease in mass (increase in  $f$ ). There is no net measurable dissipation shift as a completely formed sBLM is very compact and couples strongly to the motion of the QCM crystal. On the other hand, intact liposome adsorption is characterized by large dissipation shifts, as adsorbed liposomes are substantially larger and less compact structures. Thus, they can be subjected to large deformation under shear stress, resulting in increased energy dissipation.

Figs. 7a and 7b (Curves i and iii) show the  $\Delta f$  curves for liposome interactions with a QCM chip coated with PEMs having PDAC and PAH as the topmost layer, respectively. Neither curve exhibits two distinct phases, suggesting that BLM formation on PDAC and PAH does not follow the two-phase process reported for silicon dioxide [77]. The  $\Delta f$  value measured on PDAC ( $-95 \pm 10$  Hz) lies between  $-26 (\pm 4)$  Hz and  $-110 (\pm 10)$  Hz, values generally observed for a completely formed bilayer and for intact liposomes of similar size, respectively. This result, and also the large dissipation shift ( $4.5 \times 10^{-6}$ ) corresponding to liposome adsorption (Fig. 7a, Curve ii), suggest

that most of the liposomes on PDAC remain intact and do not rupture to form a bilayer. The previously described FRAPP results on PDAC, which showed about 22% mobile fraction, are also consistent with this hypothesis.

In contrast, liposome adsorption on PAH (Fig. 7b) resulted in a comparatively smaller frequency change (Curve iii,  $-45 \pm 10$  Hz) and dissipation shift (Curve iv,  $1.2 \times 10^{-6} \pm 0.1 \times 10^{-6}$ ). These results, together with the FRAPP results, which showed about 68% mobile fraction on PAH, suggest that most of the liposomes on PAH fused to form a BLM.

The results presented above indicate that this novel method offers several advantages over previously reported methods used to create sBLM microarrays. The use of  $\mu$ CP affords precise control over the 2-D geometry of the array at the micron (and potentially sub-micron) scale. The use of a PEM layer between the underlying surface and the biomimetic interface adds versatility, because PEM can be adsorbed to virtually any surface and because the PEM layer could serve as a hydrophilic reservoir needed for some membrane proteins to function properly. This approach also provides greater control over the physical and chemical properties of the biomimetic interface, because (1) the thickness of the PEM reservoir can be controlled with nanometer precision via the number of polyelectrolyte layers deposited, (2) the diverse range of PEMs available allows the chemical properties of the reservoir to be customized, (3) the strength of liposome deposition can be controlled, based on charge or the use of m-dPEG acid, and (4) the degree to which adsorbed liposomes rupture to form BLM can be controlled via the chemical properties of the top polyelectrolyte layer.

#### 4. Conclusions

We have developed an approach for fabricating arrays of BLMs and liposomes on PEMs that entails (1) establishing a patterned microarray of PEM and/or m-dPEG acid on a surface and (2) selectively depositing liposomes on either the features or the background of the pattern. TIRFM and fluorescence microscopy results indicated that liposomes composed of DOPA and DOPC adsorb strongly on PDAC and PAH surfaces but only weakly on SPS and poly(ethylene glycol) (m-dPEG acid) coated surfaces. We exploited these tendencies to create clean, patterned microarrays of BLMs and liposomes on PAH and PDAC. The mechanism of liposome rupture and bilayer formation is not yet fully understood. However, FRAPP and QCM results suggest that a higher fraction of liposomes rupture to form bilayers on PAH surfaces than on PDAC, where a significant percentage of the adsorbed lipids are essentially immobile.

The versatility of the approach is illustrated by its unique ability to form clean microarrays in both positive and negative image of the  $\mu$ CP stamp. Potential applications include novel biosensors and biocatalysts, microarrays for high-throughput screening of compounds that interact with cell membranes, and micropatterned interfaces to study, and possibly controlling, interactions between living cells and synthetic membranes.

## Acknowledgments

This work was funded by the NSF, the MSU Foundation and the Michigan Technology Tri-Corridor program of the Michigan Economic Development Corporation.

## References

- [1] S. Heysel, H. Vogel, M. Sanger, H. Sigrist, *Protein Sci.* 4 (1995) 2532.
- [2] D.P. Nikolelis, T. Hianik, U.J. Krull, *Electroanalysis* 11 (1999) 7.
- [3] B. Raguse, V. Braach-Maksvytis, B.A. Cornell, L.G. King, P.D.J. Osman, R.J. Pace, L. Wiczorek, *Langmuir* 14 (1998) 648.
- [4] E. Sackmann, *Science* 271 (1996) 43.
- [5] M. Stelzle, G. Weissmuller, E. Sackmann, *J. Phys. Chem.* 97 (1993) 2974.
- [6] A.L. Plant, *Langmuir* 15 (1999) 5128.
- [7] K. Asaka, A. Ottova, H.T. Tien, *Thin Solid Films* 354 (1999) 201.
- [8] S.G. Boxer, *Curr. Opin. Chem. Biol.* 4 (2000) 704.
- [9] G. Favero, A. D'Annibale, L. Campanella, R. Santucci, T. Ferri, *Anal. Chim. Acta* 460 (2002) 23.
- [10] A. Graneli, J. Rydstrom, B. Kasemo, F. Hook, *Langmuir* 19 (2003) 842.
- [11] E.E. Ross, B. Bondurant, T. Spratt, J.C. Conboy, D.F. O'Brien, S.S. Saavedra, *Langmuir* 17 (2001) 2305.
- [12] H.T. Tien, A.L. Ottova, *Electrochim. Acta* 43 (1998) 3587.
- [13] G. Wiegand, N. Arribas-Layton, H. Hillebrandt, E. Sackmann, P. Wagner, *J. Phys. Chem. B* 106 (2002) 4245.
- [14] E. Kalb, S. Frey, L.K. Tamm, *Biochim. Biophys. Acta* 1103 (1992) 307.
- [15] K. Ariga, Y. Okahata, *J. Am. Chem. Soc.* 111 (1989) 5618.
- [16] H.T. Tien, R.H. Barish, L.Q. Gu, A.L. Ottova, *Anal. Sci.* 14 (1998) 3.
- [17] W. Hoppe, W. Lohmann, *Biophysics*, Springer-Verlag, Berlin, 1983.
- [18] B.A. Cornell, G. Krishna, P.D. Osman, R.D. Pace, L. Wiczorek, *Biochem. Soc. Trans.* 29 (2001) 613.
- [19] G. Krishna, J. Schulte, B.A. Cornell, R. Pace, L. Wiczorek, P.D. Osman, *Langmuir* 17 (2001) 4858.
- [20] P. Kryszinski, A. Zebrowska, A. Michota, J. Bukowska, L. Becucci, M.R. Moncelli, *Langmuir* 17 (2001) 3852.
- [21] M.R. Moncelli, L. Becucci, S.M. Schiller, *Bioelectrochemistry* 63 (2004) 161.
- [22] J.C. Munro, C.W. Frank, *Langmuir* 20 (2004) 3339.
- [23] C.A. Naumann, O. Prucker, T. Lehmann, J. Ruhe, W. Knoll, C.W. Frank, *Biomacromolecules* 3 (2002) 27.
- [24] R. Naumann, S.M. Schiller, F. Giess, B. Grohe, K.B. Hartman, I. Karcher, I. Koper, J. Lubben, K. Vasilev, W. Knoll, *Langmuir* 19 (2003) 5435.
- [25] R. Naumann, E.K. Schmidt, A. Jonczyk, K. Fendler, B. Kadenbach, T. Liebermann, A. Offenhausser, W. Knoll, *Biosens. Bioelectron.* 14 (1999) 651.
- [26] V. Proux-Delrouyre, C. Elie, J.M. Laval, J. Moiroux, C. Bourdillon, *Langmuir* 18 (2002) 3263.
- [27] E.K. Sinner, W. Knoll, *Curr. Opin. Chem. Biol.* 5 (2001) 705.
- [28] P. Yin, C.J. Burns, P.D.J. Osman, B.A. Cornell, *Biosens. Bioelectron.* 18 (2003) 389.
- [29] R. Kugler, W. Knoll, *Bioelectrochemistry* 56 (2002) 175.
- [30] S. Moya, W. Richter, S. Leporatti, H. Baumler, E. Donath, *Biomacromolecules* 4 (2003) 808.
- [31] U.A. Perez-Salas, K.M. Faucher, C.F. Majkrzak, N.F. Berk, S. Krueger, E.L. Chaikof, *Langmuir* 19 (2003) 7688.
- [32] L. Zhang, R. Vidu, A.J. Waring, R.I. Lehrer, M.L. Longo, P. Stroeve, *Langmuir* 18 (2002) 1318.
- [33] L.Q. Zhang, M.L. Longo, P. Stroeve, *Langmuir* 16 (2000) 5093.
- [34] C. Ma, M.P. Srinivasan, A.J. Waring, R.I. Lehrer, M.L. Longo, P. Stroeve, *Colloids Surf. B* 28 (2003) 319.
- [35] M.P. Srinivasan, T.V. Ratto, P. Stroeve, M.L. Longo, *Langmuir* 17 (2001) 7951.
- [36] T. Cassier, A. Sinner, A. Offenhausser, H. Mohwald, *Colloids Biointerfaces* 15 (1999) 215.
- [37] S. Terrettaz, M. Mayer, H. Vogel, *Langmuir* 19 (2003) 5567.
- [38] U. Sohling, A.J. Schouten, *Langmuir* 12 (1996) 3912.
- [39] L.Q. Zhang, C.A. Booth, P. Stroeve, *J. Colloid Interface Sci.* 228 (2000) 82.
- [40] O.P. Tiourina, I. Radtchenko, S.B. Sukhorukov, H. Mohwald, *J. Membr. Biol.* 190 (2002) 9.
- [41] J.S. Hovis, S.G. Boxer, *Langmuir* 16 (2000) 894.
- [42] L. Kam, S.G. Boxer, *J. Biomed. Mater. Res.* 55 (2001) 487.
- [43] L.A. Kung, L. Kam, J.S. Hovis, S.G. Boxer, *Langmuir* 16 (2000) 6773.
- [44] J. Saccani, S. Castano, B. Desbat, D. Blaudez, *Biophys. J.* 85 (2003) 3781.
- [45] J.T. Groves, S.G. Boxer, *Acc. Chem. Res.* 35 (2002) 149.
- [46] J.T. Groves, S.G. Boxer, H.M. McConnell, *Proc. Natl. Acad. Sci. USA* 95 (1998) 935.
- [47] J.T. Groves, N. Ulman, S.G. Boxer, *Science* 275 (1997) 651.
- [48] L.A. Kung, J.T. Groves, N. Ulman, S.G. Boxer, *Adv. Mater.* 12 (2000) 731.
- [49] G. Decher, J.D. Hong, *Ber. Bunsen-Ges.* 95 (1991) 1430.
- [50] A. Kumar, G.M. Whitesides, *Abstr. Pap. Am. Chem. Soc.* 206 (1993) 172.
- [51] X. Jiang, P.T. Hammond, *Langmuir* 16 (2000) 8501.
- [52] X. Jiang, H. Zheng, G. Shoshna, P.T. Hammond, *Langmuir* 18 (2002) 2607.
- [53] A.C. Fou, M.F. Rubner, *Macromolecules* 28 (1995) 7115.
- [54] I. Lee, H. Zheng, M.F. Rubner, P.T. Hammond, *Adv. Mater.* 14 (2002) 572.
- [55] H. Zheng, I. Lee, M.F. Rubner, P.T. Hammond, *Adv. Mater.* 14 (2002) 569.
- [56] J.S. Ahn, P.T. Hammond, M.F. Rubner, I. Lee, *Colloids Surf. A* 259 (2005) 45.
- [57] Y. Lvov, K. Ariga, I. Ichinose, T. Kunitake, *J. Am. Chem. Soc.* 117 (1995) 6117.
- [58] I. Lee, P.T. Hammond, M.F. Rubner, *Chem. Mater.* 15 (2003) 4583.
- [59] P.M. St. John, H.G. Craighead, *Appl. Phys. Lett.* 68 (1996) 1022.
- [60] Y. Xia, E. Kim, M. Mrksich, G.M. Whitesides, *Chem. Mater.* 8 (1996) 601.
- [61] X.M. Yang, D.A. Tryk, K. Hasimoto, A. Fujishima, *Appl. Phys. Lett.* 69 (1996) 4020.
- [62] N. Kohli, P. Dvornic, S. Kaganove, M. Worden, I. Lee, *Macromol. Rapid Commun.* 25 (2004) 935.
- [63] N. Kohli, R.M. Worden, I. Lee, *Chem. Commun.* 3 (2005) 316.
- [64] I. Lee, J. Ahn, T. Hendericks, M.F. Rubner, P.T. Hammond, *Langmuir* 20 (2004) 2478.
- [65] D. Yoo, S.S. Shiratori, M.F. Rubner, *Macromolecules* 31 (1998) 4309.
- [66] S. Kidambi, C. Chan, I. Lee, *J. Am. Chem. Soc.* 126 (2004) 4697.
- [67] A. Gajraj, R.Y. Ofoli, *Langmuir* 16 (2000) 4279.
- [68] J.R. Silvius (Ed.), *Lipid-Protein Interactions*, Wiley, New York, 1982.
- [69] J.M. Harris, *Poly(ethylene glycol) Chemistry: Biotechnical and Biomedical Applications*, Plenum, New York, 1992.
- [70] K. Feldman, G. Hahner, N.D. Spencer, P. Harder, M. Grunze, *J. Am. Chem. Soc.* 121 (1999) 10134.
- [71] H.J. Kreuzer, R.L.C. Wang, M. Grunze, *J. Am. Chem. Soc.* 125 (2003) 8384.
- [72] L.L. Wright, A.G. Palmer, N.L. Thompson, *Biophys. J.* 54 (1988) 463.
- [73] B.A. Smith, H.M. McConnell, *Proc. Natl. Acad. Sci. USA* 75 (1978) 2759.
- [74] P.F. Fahey, W.W. Webb, *Biochemistry* 17 (1978) 3046.
- [75] P. Nollert, H. Kiefer, F. Jahng, *Biophys. J.* 69 (1995) 1447.
- [76] G.B. Luo, T.T. Liu, X.S. Zhao, Y.Y. Huang, C.H. Huang, W.X. Cao, *Langmuir* 17 (2001) 4074.
- [77] C.A. Keller, B. Kasemo, *Biophys. J.* 75 (1998) 1397.
- [78] P.A. Ohlsson, T. Tjarnhage, E. Herbai, S. Lofas, G. Puu, *Bioelectrochem. Bioenerg.* 38 (1995) 137.